THE ASTROPHYSICAL JOURNAL, 353:181–192, 1990 April 10

IONIZED CARBON IN SIDE-ILLUMINATED MOLECULAR CLOUDS

R. T. BOREIKO, A. L. BETZ, AND J. ZMUIDZINAS
Space Sciences Laboratory, University of California, Berkeley
Received 1989 June 12; accepted 1989 October 11

ABSTRACT

We have observed the $^2P_{3/2}$–$^2P_{1/2}$ fine-structure line of C II at 1900 GHz in five sources with ionization fronts nearly perpendicular to the plane of the sky. The LSR velocity of the C II emission is generally in good agreement with that observed for molecular species such as CO. However, the observed line widths of 3–14 km s^{-1} are typically wider than those of molecular lines and often show rapid spatial variations in the regions observed. In some sources this may indicate that part of the C II emanates from an ionized gas component, while for others it suggests an association between C II emission and an outflow. The C II brightness temperatures are typically equal to or slightly higher than the dust temperature at all locations observed. In the optically thin approximation, C II excitation temperatures are ≥ 100 K and column densities are $\leq 10^{18}$ cm^{-2} for all sources except M17, which has a more intense and complicated line profile with a larger spatial extent than any other source observed. The quoted column density estimates derived in the optically thin limit appear to be somewhat lower than those predicted by models of photodissociation regions for sources with a side-illuminated geometry, but uncertainties in the UV flux and geometry of the ionization front preclude a definitive comparison. The estimated column densities would be higher if the C II emission were somewhat optically thick, in which case the ionized carbon would be more in equilibrium with the dust at temperatures lower than predicted by current models.

Subject headings: infrared: spectra — interstellar: molecules — nebulae: structure

I. INTRODUCTION

The initiation of star formation in the depths of cold molecular clouds brings about a distinct upheaval in the region. The high UV and optical flux emitted from first-generation stars disturbs the parent molecular material, and the disruptive energetics may trigger the formation of a subsequent generation of stars in the cloud. The interface between the hot, UV-ionized H II region and the colder molecular material is delineated by the presence of both neutral atomic gas and ionized species with ionization potentials less than the 13.6 eV of hydrogen. An important constituent of such photodissociation regions is singly ionized carbon (C II), because carbon is both abundant and has an ionization potential 2.3 eV below that of hydrogen. Models of photodissociation regions, such as those of Glassgold and Langer (1974), Langer (1976), and Tielens and Hollenbach (1985), predict that radiation from the $^2P_{3/2}$–$^2P_{1/2}$ fine-structure line of C II at 1900 GHz (158 μm) will provide the major cooling for intermediate-density regions and consequently should be quite intense. This prediction has been confirmed by observations of the 158 μm line in several molecular clouds (e.g., Russell *et al.* 1980, 1981; Melnick *et al.* 1986; Crawford *et al.* 1986). However, with the exception of the recent heterodyne observations of Orion (Boreiko, Betz, and Zmuidzinas 1989), previous C II spectra were of limited spectral resolution so that only the integrated intensity and in some cases the approximate line width could be determined, but without any detailed information on the shape of the line profile. Line shapes and resolved peak intensity (T_A^*) measurements are important for determining lower limits to excitation temperature and allow direct comparison with resolved profiles from other species such as CO which trace conditions in the neighboring molecular gas.

In this paper we present the results of observations of the $^2P_{3/2}$–$^2P_{1/2}$ line of C II obtained with a laser heterodyne spectrometer operating at 0.8 km s^{-1} resolution, which is well matched to the smallest velocity dispersions expected in molecular clouds. For this first study, five sources with ionization fronts observed "edge-on" were selected. By "edge-on" we mean that the source of the ionization is external to the molecular cloud (and not necessarily formed from it) and is angularly separated from the molecular region in the plane of the sky. This geometry is convenient for studying the ionization front and the variation of parameters with distance from the ionizing source without confusion from emission from the front and back parts of an ionized shell. Also, it is the geometry which maximizes the column density for tangential views and hence is most likely to lead to optically thick C II radiation and thereby yield a good estimate for the excitation temperature of the photodissociation region. Some of the objects observed also contain one or more embedded UV-sources and offer the opportunity to compare photodissociation regions formed under different conditions. In these sources with different angles of view available, one might expect a greater C II column density in the side-illuminated regions than in areas foreground to the embedded source. Regardless, in all cases, resolved line profiles for the photodissociation region will give valuable information on the cloud kinematics when compared to line shapes derived independently from the molecular gas (e.g., those of CO).

II. INSTRUMENTATION AND CALIBRATION

The instrument used for the observations discussed here is an airborne far-infrared heterodyne receiver which has been described in detail by Betz and Zmuidzinas (1984). For observations of C II at 1900.5369 GHz (Cooksy, Blake, and Saykally 1986), the local oscillator is an optically pumped CH_2F_2 laser operating at 1891.2743 GHz (Petersen, Scalabrin, and Evenson 1980), thereby yielding an IF centered at 9.3 GHz. The mixer, a GaAs Schottky diode in a corner-reflector mount (Zmuidzinas, Betz, and Boreiko 1989), was operated uncooled in 1987 and

cooled to 77 K in 1988. The "back end" consists of two filter banks in parallel: one with 40 channels of 5 MHz (0.8 km s^{-1}) resolution covering a 32 km s^{-1} range and the other with 64 channels of 20 MHz (3.2 km s^{-1}) resolution spanning 200 km s^{-1}. The wider bandwidth filter bank provides a clear continuum level, while the narrow filter bank gives the high-resolution C II profile.

Since the Earth's atmosphere is essentially opaque from ground level at the C II frequency, the instrument was flown aboard NASA's Kuiper Airborne Observatory at an altitude of 12.5 km, where typically the atmospheric transmission is better than 90%. The telescope beam width was measured from a scan of the lunar limb to be ~43″ FWHM and the coupling efficiency was measured to be ~0.6 for all observations. The telescope secondary was chopped at 2 Hz with an amplitude of 10′, which is sufficient to prevent significant contamination from line emission in the reference beam for all sources except M17. The direction of chop was perpendicular to the ionization front for all of the edge-illuminated objects.

Most of the observations discussed in this paper were obtained in a single flight on 1987 July 28 with a system noise temperature T_{sys} = 30,000 K (SSB). The sources Cep A and Cep B had also been observed earlier on 1987 February 9 with a 6′.5 chopper throw and T_{sys} = 35,000 K (SSB), while S201 was observed later on 1988 February 2 with T_{sys} = 26,000 K (SSB). Calibration in 1987 February and 1988 February was obtained from measurements of the moon, which was assumed to have a physical temperature of 394 K and an emissivity of 0.98 (Linsky 1973). The double- to single-sideband conversion was calculated from the known transmissions of the atmosphere and the aircraft pressure window in the two sidebands. The primary calibration was maintained throughout the flight by periodic observations of a blackbody source which was used as a secondary standard. The moon was not available for direct calibration during the 1987 July flight, and therefore only the secondary standard was used, and the blackbody temperature was assumed to be the same as for the 1987 February flight. An independent check on this procedure was derived from measurements of the strong C II line in Cep B: the same location was observed in both 1987 July and 1987 February, and the measured antenna temperatures of the resulting spectra were identical to within 5% (which is the statistical uncertainty). The net uncertainty in the calibration for a uniform source filling our beam is estimated to be $\leq$10%. Pointing accuracy is ~15″. The velocity scale, determined from the line and LO frequencies, is accurate to better than 0.4 km s^{-1}.

III. OBSERVATIONS AND ANALYSIS

Two or more locations in five sources having edge-illuminated ionization fronts (S140, S201, NGC 7538, Cep B, and M17) were observed in an attempt to determine the general properties of C II radiation from photodissociation regions at the edges of molecular clouds. The parameters of the observed lines are given in Table 1. The continuum temperature is determined from an average of the data in the 64 × 20 MHz filter bank excluding those channels with line radiation, and has been corrected to a SSB value. No significant slope or baseline standing waves were found in any of the spectra. The channel-to-channel variations outside the line profile are consistent with those expected from the quoted system noise temperatures. The antenna temperature of the line has been corrected for the continuum level and, along with V_{LSR} and FWHM, is determined from a fit of a Gaussian line profile to the data. In spectra for which a single Gaussian is not an adequate representation, several Gaussians are fitted, and the parameters for each of the components are listed. The inte-

TABLE 1

OBSERVED C II LINE PARAMETERS

Position	T_A^*[a] (K)	T_B[b] (K)	V_{LSR} (km s^{-1})	ΔV_{FWHM} (km s^{-1})	$I_{INT} \times 10^{-4}$ (ergs cm^{-2} s^{-1} sr^{-1})	T_{CON}[c] (K)
S140–IRS	8.0(1.0)	36.2(1.7)	−6.8(0.4)	6.5(0.9)	3.6(0.6)	1.05(0.09)
S140–30″ SW	17.5(2.0)	50.0(2.6)	−8.3(0.2)	3.5(0.4)	4.6(0.6)	0.67(0.13)
S201–FIR	7.4(0.4)	35.2(0.7)	−38.0(0.2)	7.4(0.5)	4.2(0.4)	0.04(0.05)
S201–1′ SW	14.2(1.5)	45.5(2.1)	−37.3(0.2)	3.7(0.4)	4.0(0.5)	0.35(0.11)
NGC 7538–IRS1	11.6(1.0)	41.8(1.5)	−57.5(0.6)	13.7(1.5)	11.6(1.0)	0.42(0.18)
NGC 7538–1′ NW	16.1(0.7)	48.1(0.9)	−57.0(0.2)	9.3(0.5)	12.4(0.7)	0.17(0.08)
Cep B–FIR	28.0(0.9)	63.0(1.1)	−13.9(0.1)	4.2(0.1)	9.0(0.5)	0.35(0.08)
Cep B–1′ NW	21.3(2.0) 5.3(1.5)	54.8(2.5) 31.4(2.9)	−13.7(0.1) −16.5(1.2)	3.2(0.3) 8.7(1.5)	8.4(0.6)	0.00(0.12)
Cep B–2′ NW	5.5(0.9)	31.8(1.7)	−15.8(0.5)	6.7(1.3)	2.1(0.6)	−0.16(0.11)
M17–C II peak	31.2(2.3) −10.7(1.9) −11.1(2.2)	66.7(2.7) 40.5(2.9) 41.1(3.3)	19.4(0.2) 21.2(0.1) 17.8(0.4)	13.0(0.4) 1.7(0.3) 5.5(1.1)	24.4(0.4)	0.80(0.07)
M17–Mid	26.3(1.2) −10.6(2.5)	60.9(1.4) 40.3(3.8)	19.2(0.2) 20.8(0.2)	12.4(0.5) 1.8(0.6)	23.4(0.7)	1.21(0.11)
M17–C I peak	33.1(4.4) −24.0(3.8)	68.9(5.1) 58.2(4.7)	19.3 21.2(0.3)	10.5(0.6) 5.9(0.6)	15.4(0.7)	0.67(0.11)

NOTE.—Values in parentheses represent 1 σ statistical uncertainties.

[a] T_A^* is corrected for the continuum. Negative values of T_A^* represent absorption or reference beam emission; the associated values of T_B apply in the case of reference beam emission only.

[b] T_B is brightness temperature.

[c] The continuum temperatures are corrected for transmission of the pressure window in each of the two infrared sidebands, and represent SSB values.

grated intensity is not derived from the fitted parameters and thus represents the total value for all components. In the following sections, the spectra from individual sources are presented and discussed in detail.

a) *S140*

S140 is a source with an apparently simple geometry which minimizes possible confusion in the interpretation of data. The dense molecular cloud core contains several embedded IR sources, and is surrounded by an extended dark cloud and CO envelope (Blair *et al.* 1978). Toward the SW is an Hα rim, and an ionization front exists ~2.5 SW of the embedded sources (Hayashi *et al.* 1985). The primary exciting star for the H II region is a B0 star 7′ SW of the Hα rim, and therefore S140 is a clear-cut example of a source in which the primary ionization front is seen "edge-on". Schematic illustrations of the morphology are given by Blair *et al.* (1978, Fig. 10) and Lester *et al.* (1986, Fig. 1).

Observations in several molecular transitions show that the emission from neutral gas generally peaks near S140 IR, with a sharp cutoff toward the ionization front (CS: Snell *et al.* 1984; Hayashi *et al.* 1985; Mundy *et al.* 1986; CO: Blair *et al.* 1978; Hayashi *et al.* 1987). There is little systematic change of V_{LSR} with position in S140, but the line width shows a general decrease away from the ionization front (Snell *et al.* 1984). LVG modeling of CS data (Snell *et al.* 1984; Mundy *et al.* 1986) indicates that the gas has a maximum density of $\sim 10^6$ cm^{-3} in the SW near the interface with the H II region and decreases toward the NE, and that this gas is clumpy, with the high-density component immersed in a more tenuous extended medium. The foreground or interclump gas has densities of 4×10^3 to 4×10^5 cm^{-3} (Mundy *et al.* 1987) with a velocity dispersion similar to that of the clumps, since no self-reversals are seen in the profiles. The mean kinetic temperature at S140 IR is ~35 K as derived from CO (Blair *et al.* 1978) and NH_3 (Takano 1986) observations.

We obtained C II spectra of S140 at two locations: the embedded sources (S140 IR) and 30″ SW, in the direction toward the ionization front. As can be seen from the parameters listed in Table 1, the C II emission is stronger closer to the ionization front than at S140 IR, as expected. However, the difference in peak T_A^* of the emission at the two nearby locations is accompanied by a compensating factor of ~2 change in line width, such that the integrated intensity in the line is very nearly constant. The C II emission from S140 IR probably originates from the ionization region thought to exist around at least two of the embedded sources (Schwartz *et al.* 1983), which are likely to be early B stars. The greater width of the C II line could be due to increased turbulence in the photodissociation region surrounding the embedded sources compared with that in the ionization front. The CO lines show a marked blue asymmetry and increased line width at IRS compared to other locations (Blair *et al.* 1978; Hayashi *et al.* 1987), and the extended wings seen in ^{12}CO and ^{13}CO (Snell *et al.* 1984) have been interpreted as evidence of an outflow. The C II line profile appears quite similar to that of $J = 2$–1 ^{12}CO (see Fig. 1), with the exception of the apparent absence of the extended blue wing in the C II data. Therefore the outflow could be affecting the photodissociated gas to some extent, producing wider lines than at the ionization front. This interpretation is reminiscent of observations of C II in the Orion region (Boreiko, Betz, and Zmuidzinas 1987) which show greater line width toward BN-KL than near the Trapezium, though the C II line wings do not have the large velocity width seen in CO observations.

An alternative interpretation for the width of the C II line might be based on optical depth considerations similar to those used for CO: the ^{13}CO line width is ~60% of that of ^{12}CO, while C^{18}O produces lines narrower still, suggesting that optical depth may contribute significantly to the observed width. However, given the complicated nature of radiative transfer in an inhomogeneous cloud and the rapid spatial

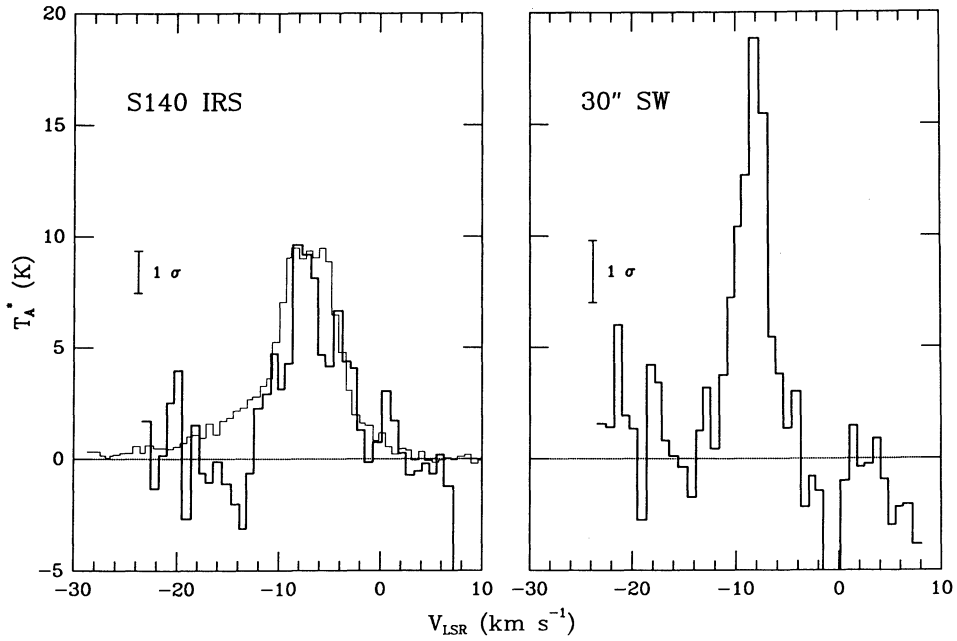

FIG. 1.—C II spectra in the S140 region. *Left panel:* C II at IRS (*heavy line*) compared with CO $J = 2$–1 (*light line:* Plambeck, Snell, and Loren 1983; scaled by 0.5). *Right panel:* C II 30″ SW of IRS. Integration times are 8 minutes at IRS and 4 minutes 30″ SW. The continuum determined from the wide filter bank has been subtracted from both C II spectra.

variation of line profile seen (and qualitatively expected as the dominant heating changes from an internal source associated with an outflow to an external one), it is impossible to draw any firm conclusions on the role of optical depth in producing the observed line width. Only a 1 σ upper limit to τ of ~ 10 (for an assumed isotopic ratio of 60) can be placed by the nondetection of the ^{13}C II hyperfine component at $+11.2$ km s^{-1} relative to the ^{12}C II line.

The C II column density at IRS in the optically thin high temperature ($T > 150$ K) limit is 2.3×10^{17} cm^{-2}, a factor of 3–10 smaller than that obtained from photodissociation models for H_2 densities between 10^3 and 10^6 cm^{-3} and UV fluxes between 10^3 and 10^5 times the interstellar flux (Tielens and Hollenbach 1985). Possible beam dilution may be partly responsible for the comparatively low measured value of the integrated intensity and derived column density, since the photodissociated region produced by the embedded sources within the molecular cloud is expected to be compact. In addition, the flux of ionizing radiation is not known at this location, although because of the nearby UV source it is probably within the range quoted above for which the C II column density is not predicted to be very sensitive to UV flux. A lower limit of 36 ± 2 K for T_{ex} can be derived from the peak line strength. Partial beam filling would tend to raise this limit.

The C II line profile at the position 30″ SW of the embedded sources (see Fig. 1) is considerably narrower and brighter than at IRS, but with a similar integrated intensity. The position observed is about midway between IRS and the ridge of heated molecular gas seen in CO inside the ionization front (Hayashi *et al.* 1987), which corresponds with the sharp drop-off in intensity in other species such as CS. The dust temperature reaches a local minimum value of ~ 40 K near this location, marking the cross-over point between heating from the embedded sources and the external ionizing star (Lester *et al.* 1986). The brightness temperature of the C II at this position is 50 K, and the minimum column density of C II in the high-temperature limit is 3×10^{17} cm^{-2}, similar to that at IRS. It is likely that the photodissociation in this region is produced by UV from the external star after considerable attenuation by dust and other molecular material. Therefore, the UV flux parameter G_0 will be significantly less than the value of 150 calculated by Keene *et al.* (1985) at the ionization front. Available PDR models do not explicitly predict observable C II intensities for these low values of G_0, but extrapolation of the trend in integrated intensity with G_0 shown in the model of Tielens and Hollenbach (1985) suggests, as expected, that the observed value could be obtained with an appropriate lower value of G_0. A stronger C II line would be expected closer to the ionization front, and measurements of the minimum column density and brightness temperature at various points in this direction would be informative for determining the relative roles of the embedded and external sources in C II production.

b) S201

S201 is a small ($\sim 6'$), bright H II region embedded in a molecular cloud extending westward at least 12′ to the edge of W5. Visually, it has a highly structured and bipolar appearance produced by an E-W lane of obscuration from either foreground material or higher density neutral gas intermixed with the ionized gas. Radio continuum observations (Felli, Hjellming, and Cesaroni 1987) with 6″ resolution show a bright and almost unresolved ridge at the eastern end of S201, almost coincident with the brightest optical region. Felli, Hjellming, and Cesaroni modeled the radio continuum data convincingly as a spherical molecular cloud which is illuminated and ionized by an early-type (O9) star that is to the west of the cloud and external to it almost in the plane of the sky. This interpretation is supported by the infrared observations of Mampaso *et al.* (1989). Thus, based on this model, S201 is also a good example of a source in which the ionization front is seen almost edge-on. Only the molecular cloud east of the star shows an ionization front, while the extensive molecular cloud to the west appears to be beyond the Strömgren radius of the ionizing star.

Mapping in CO (Martin and Barret 1978; Wramdemark and Lynga 1987; Snell *et al.* 1988) shows an elongated E-W structure with two distinct peaks in excitation temperature, separated by $\sim 5'$, one on either side of the H II region. The brightest (western) peak has $T_{ex} \sim 24$ K, and the secondary (eastern) peak shows $T_{ex} \sim 18$ K, near but not coincident with the ionization front. The line shape in CO is highly variable spatially and has a weak secondary feature visible at some locations.

Mapping in the far-infrared (FIR) continuum (Thronson *et al.* 1984) shows a single peak near the ionization front with a FWHM $\sim 50''$ and extended lower contours. The dust temperature is ~ 42 K at the observed peak, dropping slowly to 30–35 K 3′ to the west. This range of dust temperatures is in good agreement with that predicted by Felli and Harten (1981) under the assumption that the dust is heated by an O9 V star within the positional uncertainty of the infrared source AFGL 416. Densities in the region are fairly low: Martin and Barret (1978) obtained an average density of 2.4×10^3 cm^{-3}, while Thronson *et al.* (1984) calculate a peak density of $\sim 10^4$ cm^{-3} in the east, with possibly slightly higher values at the western CO peak. A schematic representation of S201 is presented by Mampaso *et al.* (1989, Fig. 1).

Our C II observations were made at two locations in the S201 region. The first is at the FIR peak of Thronson *et al.* (1984), where the 43″ beam size encompasses the ionization front, the location of the proposed ionizing star, and the eastern peak of CO column density, although not the location of peak CO excitation temperature. The second location is 1′ to the SW along a line joining the two peak positions seen in radio continuum data (Felli, Hjellming, and Cesaroni 1987). At this second location, which is closer to the center of the visible H II region, radio continuum emission is weak, and the ^{13}CO column density is near a local minimum between the eastern and western peaks. The CO excitation temperature at our two observed locations is ~ 15 K, with the FIR peak being in a high gradient region while the position 1′ SW is close to the rather extended local minimum between the two CO peaks. The dust temperature is near 40 K at both positions. The C II spectra we observed are shown in Figure 2, and the parameters deduced from Gaussian fits to the data are listed in Table 1.

As shown in Figure 2, the C II line at the FIR peak is symmetric and relatively wide. Its V_{LSR} of -38.0 ± 0.2 km s^{-1} is in fairly good agreement with that of the $J = 1$–0 line of ^{12}CO, -38.5 km s^{-1} (Snell *et al.* 1988). However, the C II line width of 7.4 ± 0.5 km s^{-1} is about a factor of 2 larger than that found for the CO line, which was observed with a similar beam size of 45″. The difference in line width could be attributed to the greater contribution to the C II emission from the ionization front, where turbulence may be enhanced over that in the molecular cloud. In the model of Felli, Hjellming, and Cesaroni (1987), material in the molecular cloud ionized by the

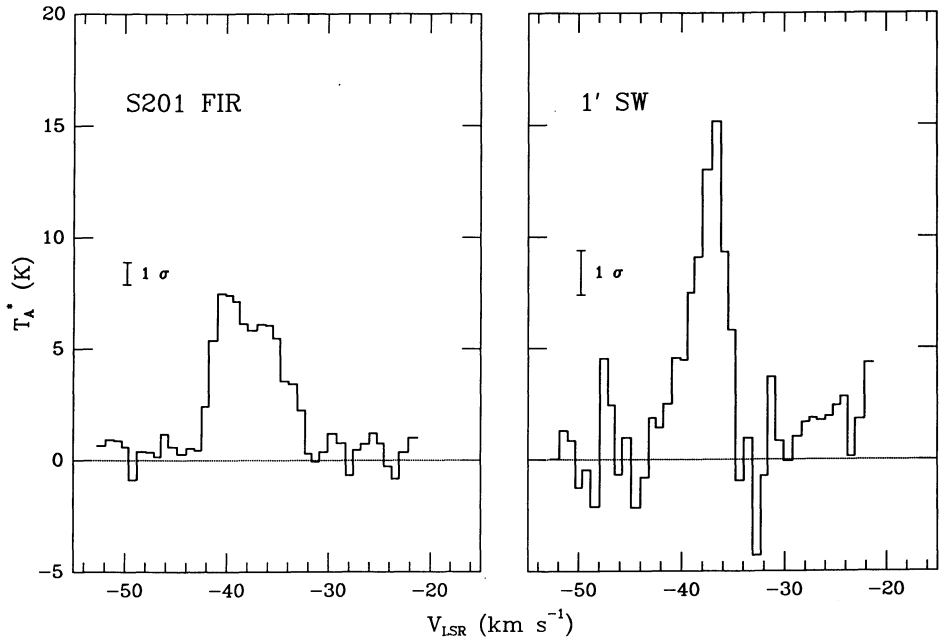

FIG. 2.—C II spectra toward S201: at the FIR peak (*left panel*, 24 minutes integration) and 1′ SW of the FIR peak (*right panel*, 6 minutes integration). The continuum determined from the wide filter bank has been subtracted from the spectra. Some residual wing emission may still be present at the limits of the high-resolution spectrum presented here.

stellar UV radiation streams away radially at the speed of sound. A significant fraction of C II line radiation may arise from this newly ionized material and contribute to the apparent width of the line. Because of the geometry of the source, no asymmetry would be expected from the streaming, and none is apparent in the observed C II profile. The brightness temperature of the C II line is $\sim$36 K, which is close to the dust temperature at this location but hotter than the CO excitation temperature. The spatial variability of CO line shape and V_{LSR} indicates complex motions within this region, which may account for the striking differences in the C II line profile between the two nearby locations that were observed. The minimum column density of C II at this location in the optically thin high temperature limit is 3×10^{17} cm^{-2}. In the optically thick limit with $T_{ex} \sim 40$ K, the minimum column density increases to $1 \times 10^{18} \tau$ cm^{-2}. The source geometry deduced from the model of Felli, Hjellming, and Cesaroni (1987) can be used to estimate G_0 to be 3000 at the ionization front. Thus for S201 the measured integrated intensity and column density are significantly lower than predicted by photodissociation region models for the appropriate conditions, especially for an ionization front oriented along the line of sight. However, beam dilution may be significant for this source which is 2–3 kpc away (Felli, Hjellming, and Cesaroni 1987). Therefore, higher spatial resolution observations are needed before any real discrepancy can be asserted.

The C II line profile 1′ SW of the FIR peak is twice as strong and half as wide as that at the FIR peak and appears to have an extended blue wing, although this latter feature is not statistically significant. The high brightness temperature of 45 K at this position is somewhat puzzling, since it is higher than that of C II at the FIR peak, where most of the C II is expected to arise. The C II emission at this location most likely originates from an interface with molecular material located behind the H II region. This interface is viewed more nearly face-on and therefore perhaps has a smaller line-of-sight velocity gradient than the material at the FIR peak, resulting in a narrower C II line. The possible extended blue wing is consistent with ionized material streaming away from the interface. Furthermore, there might be an additional source of heating in the 1′ SW region, perhaps associated with the phenomenon (possibly a shock) responsible for the peculiar CO line shapes seen further SW. Obviously, more complete mapping at high resolution, especially toward the western CO peak and the region of variable and asymmetric line shapes, will be required to understand the complex morphology of S201.

Some of the C II emission may originate from the H II region itself, since in a region ionized by an O9 star, most of the carbon can be expected to be in this ionization state. The integrated intensity of the C II line from this source can be estimated using the electron number density and H II extent deduced from the model of Felli, Hjellming, and Cesaroni (1987), and is found to be $\sim 4 \times 10^{-4}$ ergs cm^{-2} s^{-1} sr^{-1} near the ionization front and $\sim 2 \times 10^{-5}$ ergs cm^{-2} s^{-1} sr^{-1} 1′ SW, for a fractional carbon abundance of 10^{-4}. Thus, even taking into account the fact that only about half of the beam at the FIR peak falls on the H II region, a significant part of the observed radiation at this position may arise from the fully ionized hot gas rather than from an ionization front. The greater width of the line at the FIR peak compared with 1′ SW could reflect the contribution from the hot ionized gas.

c) *NGC 7538*

NGC 7538 is an H II region $\sim$5′ in diameter which is shaped like an incomplete shell; most of the thermal radio emission arises in the western section (Churchwell and Bieging 1982). There are 5 IR sources near the center of the H II region, two of which are mid-O spectral type and at least partly responsible for the ionization of the nebula (Werner *et al.* 1979). Adjacent to the H II region in the south is an extended molecular cloud bounded by the ionization front. Embedded in the cloud $\sim$2′ SE of the center of the H II region are three closely grouped

(15″) infrared sources, IRS 1–3, each accompanied by a compact H II region. Mapping in the FIR continuum (Werner *et al.* 1979) shows that the dust column density is greatest near IRS 1–3, where the derived grain temperature is $T_d \sim 45$ K. The temperature decreases slightly northward, to $T_d \sim 40$ K, before increasing again into the H II region, reaching a value of $T_d \sim 70$ K. The column density of the gas as traced by ^{13}CO also peaks near IRS 1–3, and is extended in the form of an E-W ridge (Dickel, Dickel, and Wilson 1981; Scoville *et al.* 1986). Maps in ^{12}CO and ^{13}CO show a steep gradient in column density, and to a smaller degree excitation temperature, northward from IRS 1–3, with the ridge being coincident with the boundary of the H II region. This morphology (illustrated in Fig. 2 of Dickel, Dickel, and Wilson 1981) suggests that expansion of the ionized region has compressed the molecular cloud (Campbell and Thompson 1984). Emission from vibrationally excited H_2 is also seen over a $\sim 1'$ region between the H II region and the embedded sources and is strongest $\leq 30''$ from IRS 1–3 (Fischer *et al.* 1980). It has been suggested that this emission is from shock-excited gas at the interface between the outflow and the compressed gas at the boundary with the H II region (Fischer *et al.* 1985).

Our C II observations of NGC 7538, shown in Figure 3, were made at two locations: IRS 1–3, and 1′ NW along a line joining IRS 1–3 with the center of the H II region. This latter position is on the ionization front at the interface between the H II region and the molecular cloud, where the column density and excitation temperature of CO show a steep gradient, and also includes part of the region of vibrationally excited H_2 emission. The excitation temperatures of CO are $T_{ex} \sim 22$ K and $T_{ex} \sim 18$ K at IRS 1–3 and 1′ NW, respectively (Campbell and Thompson 1984), while the dust temperature is $T_d \sim 45$ K at both locations (Werner *et al.* 1979). From Table 1 it can be seen that the brightness temperatures of C II in the two locations, 42 K and 48 K, respectively, are again similar to the dust temperature but somewhat higher than the temperature of the molecular gas. The -57 km s^{-1} V_{LSR} of the C II line at both locations corresponds to that of the molecular cloud rather than the H II region (-60 km s^{-1}, Churchwell and Bieging 1982).

Figure 3*a* shows a comparison of our observed C II spectrum (with the continuum subtracted) to the $J = 2$–1 line of CO at IRS 1–3 (G. Stacey, private communication). The agreement between line shapes is good if the different signal-to-noise ratios of the two spectra are taken into account. The extended red wing which is more evident in the CO spectrum may be a contribution from another cloud in the region: Campbell and Thompson (1984) detected at least three additional CO components with more redshifted velocities at various locations in NGC 7538. The asymmetry apparent in the CO spectrum is not obviously present in the C II data, which can be fitted by a single Gaussian component to within statistical uncertainties.

The 13.7 km s^{-1} (FWHM) width of the C II line is similar to that seen in low-J ^{12}CO lines. However, both are wider than the $\Delta V \sim 6$ km s^{-1} line width typical for ^{13}CO (Campbell and Thompson 1984) and C I (Phillips and Huggins 1981), and the $\Delta V \sim 4.5$ km s^{-1} line width observed in species requiring higher densities for excitation (e.g., CN: Churchwell and Bieging 1982; OCS: Goldsmith and Linke 1981). The IRS 1–3 region of NGC 7538 has similar physical characteristics to S140 FIR which also has embedded sources and an outflow seen in CO. Again, it is possible that the outflow in the molecular material also affects the photodissociated region, resulting in a wider line that at the ionization front. However, analogous to ^{12}CO, optical depth effects cannot be ruled out as possible contributors to the observed C II line width.

The 42 K brightness temperature of the C II line at IRS 1–3 is a lower limit to the excitation temperature because both the optical depth and beamfilling factor are unknown. However, beam dilution should be less significant in this case since the three embedded sources are spread over $\sim 15''$. The C II column density, calculated from the physical argument of

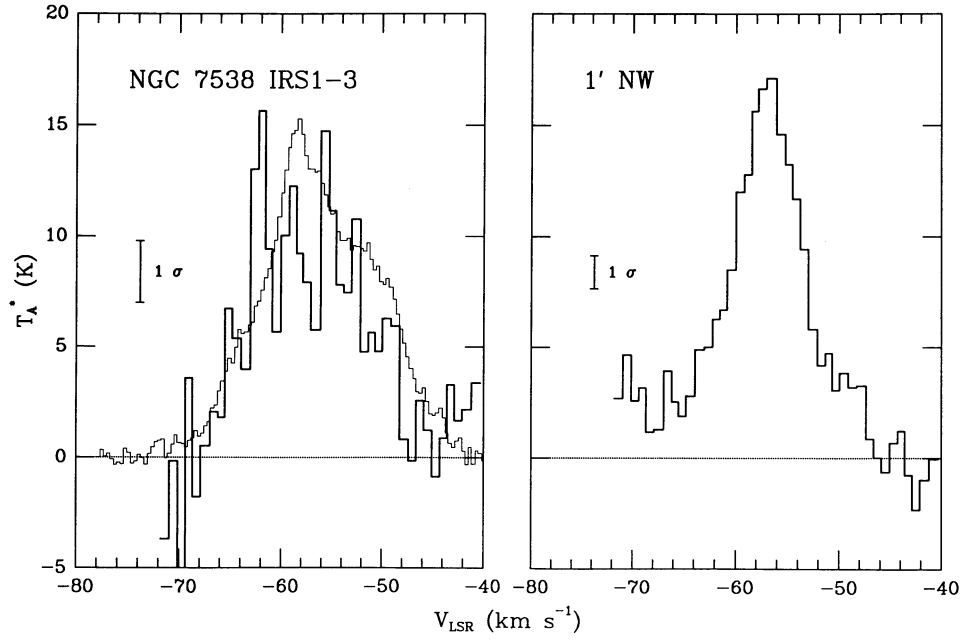

FIG. 3.—C II spectra in the NGC 7538 region. *Left panel:* C II at IRS 1–3 (*heavy line*) compared with CO $J = 2$–1 (*light line;* G. Stacey, private communication). *Right panel:* C II 1′ NW of IRS 1–3, at the ionization front. Integration times are 4 minutes at IRS 1–3 and 14 minutes 1′ NW. The continuum determined from the wide filter bank has been subtracted from the spectra.

Tielens and Hollenbach (1985) in which the photoionization of C to C^+ proceeds to a UV penetration depth of $A_v \sim 4$ (or $N_{H\,II} = 7.6 \times 10^{21}$ cm^{-2}), is $\sim 2 \times 10^{18}$ cm^{-2} for a single source of ionization when viewed collinear with the direction of ionization, and some factor < 3 greater than this for the net contribution from all three embedded sources. The minimum column density in the optically thin high temperature limit derived from the observed integrated intensity of the C II line at IRS 1–3 is 7.4×10^{17} cm^{-2}. This value is a factor of ~ 4 lower than that expected from the UV-penetration argument, but given the uncertainties such as grain parameters and dust-to-gas ratio implicit in the calculation, as well as the unknown UV flux, is not totally inconsistent with an assumption of optically thin emission. The larger C II integrated intensity in NGC 7538 compared with those from S140 and S201 may simply reflect the number, spatial distribution, and evolutionary stages (UV-output) of the embedded stars responsible for the C II ionization. On the other hand, there is no conclusive evidence to rule out the alternative limiting case of somewhat optically thick C II emission with an excitation temperature ~ 50 K, close to the dust temperature. Column densities in this latter case would be closer to the values calculated on the basis of UV penetration depths.

Figure 3*b* shows the C II line at the ionization front. Our beam at this location encompasses a region with H_2 vibrational emission, which has been interpreted as a product of shock excitation. The heating of the gas by the outflow is expected to be localized at this shock front, but should not produce a noticeable increase in line temperature averaged over our beam (Scoville *et al.* 1986). The C II line shape is well represented by a single Gaussian component with no evidence of extended wing emission to within statistical uncertainties. The brightness temperature of the line is higher than at IRS 1–3, but the integrated intensity is very similar because the line width is smaller. Thus calculated column densities in the optically thin high temperature limit are similar to those at IRS 1–3, even though the edge-on view should give a longer projected path through the ionization front at this position.

The UV flux at the ionization front correponds to $G_0 \sim 1000$ if all the UV is assumed to originate from the O7 star at IRS 6. Column densities from PDR models for this value of G_0 for an interface viewed face-on are similar to the measured value for the approximately edge-on view. However, as in the case of S201, the distance to NGC 7538 (~ 3 kpc; Churchwell and Bieging 1982) suggests that beam dilution or pointing uncertainties in the 10″–15″ range may significantly decrease the measured integrated intensity.

d) Cep B

The molecular cloud in Cepheus is located near the Galactic plane and is elongated parallel to it, extending for over 4°. The cloud consists of several components, as shown by distinct peaks in the spatial distribution of CO radiation (Sargent 1977). The Cep A region contains several embedded sources with at least three compact H II regions within a 5″ radius (Beichman, Becklin, and Wynn-Williams 1979). Line profiles from this region show the high-velocity wings characteristic of a bipolar outflow (Bally and Lada 1983). Further evidence of energetic activity in this region is provided by emission from vibrationally excited H_2 (Bally and Lane 1982). The millimeter-wave CO lines from Cep A show deep self-absorption at some locations (Sargent 1977; Phillips *et al.* 1981).

The CO radiation of highest excitation arises from a distinct region in the NW of the molecular cloud, Cep B, which forms an interface with the H II region S155. Observations in the radio continuum (Felli *et al.* 1978) show the presence of a ridge coincident with the optical bright rim at the interface with S155, with a plateau behind the ridge into the molecular cloud. Modeling of the region by Felli and coworkers (1978) indicates that the main source of molecular excitation comes from external stars which are responsible for the ionization of the H II region and are situated such that the ionization front is inclined $\sim 50°$ with respect to the plane of the sky. The far infrared continuum emission is also strongest near the interface between the molecular cloud and H II region S155 (Evans *et al.* 1981; see Fig. 1 for a schematic illustration), with the higher gradient being toward the H II region. Dust temperature appears to decrease away from the photodissociation edge of the cloud, as expected from a morphology in which the source of heating is external.

Our observations of C II in the Cepheus molecular cloud included four positions: Cep A, the FIR peak in Cep B, and locations 1′ and 2′ NW from the FIR peak in Cep B toward the H II region. Only a single 4 minute integration was obtained at Cep A. No C II emission was seen, with a 2 σ upper limit to the integrated intensity of 2.4×10^{-4} ergs cm^{-2} s^{-1} sr^{-1}. The continuum, however, was quite strong at this location, 1.2 ± 0.2 K, in good agreement with the 1.1 K expected from the measurements of Evans *et al.* (1981). The reason for the absence of C II emission at this location is not totally clear, since the presence of compact H II regions within the molecular cloud implies a surrounding photodissociation region and a consequent C^+ envelope. However, beam dilution will be quite severe, since these regions all lie within $\sim 6''$. More significantly, marked reversals are seen in the profiles of CO rotational lines, which raises the possibility that the C II emission could be self-absorbed as well, as seems to be the case in several other molecular clouds (Betz, Boreiko, and Zmuidzinas 1990). With the appropriate velocity, line width, and density or temperature gradients through a cloud, it is possible for C II emission to be completely self-absorbed and for any residuals to be masked by foreground continuum emission from the same cloud. A more definitive conclusion will require more sensitive observations of Cep A at several spatial locations.

The spectra obtained at the three positions in the Cep B-S155 region are shown in Figure 4, and the parameters deduced from Gaussian fits to the spectra are listed in Table 1. At the FIR peak, the C II line has $T_A^* = 28$ K, which implies a minimum excitation temperature of 63 K. For comparison, ^{12}CO $J = 1$–0 has $T_A^* \sim 13$ K at this position measured with a 65″ beam (Sargent 1977), and the dust temperature is 43 ± 3 K (Evans *et al.* 1981). The CO velocity structure of the Cep B region is complex, with several components evident. Most of the CO emission from the Cep B region has a V_{LSR} center of approximately -12 km s^{-1}, with a component at -15 km s^{-1} appearing only close to S155. The emission from C II appears at $V_{LSR} = -13.9$ km s^{-1}, and the 4.2 km s^{-1} (FWHM) line width of the C II is similar to the 2–4 km s^{-1} seen for CO. The minimum column density of C II at the FIR peak, assuming an optically thin line in the high temperature limit, is 5.7×10^{17} cm^{-2}. Our nondetection of the strongest hyperfine component of the ^{13}C II line places a 3 σ upper limit on the optical depth of 11 (assuming $[^{12}C]/[^{13}C] = 60$). The ^{12}C II integrated intensity measured at this location is consistent with predictions of PDR models for the geometry of the source and $G_0 \sim 650$, as deduced from the model of Felli *et al.* (1978).

At a position 1′ NW of the FIR peak in Cep B, where the

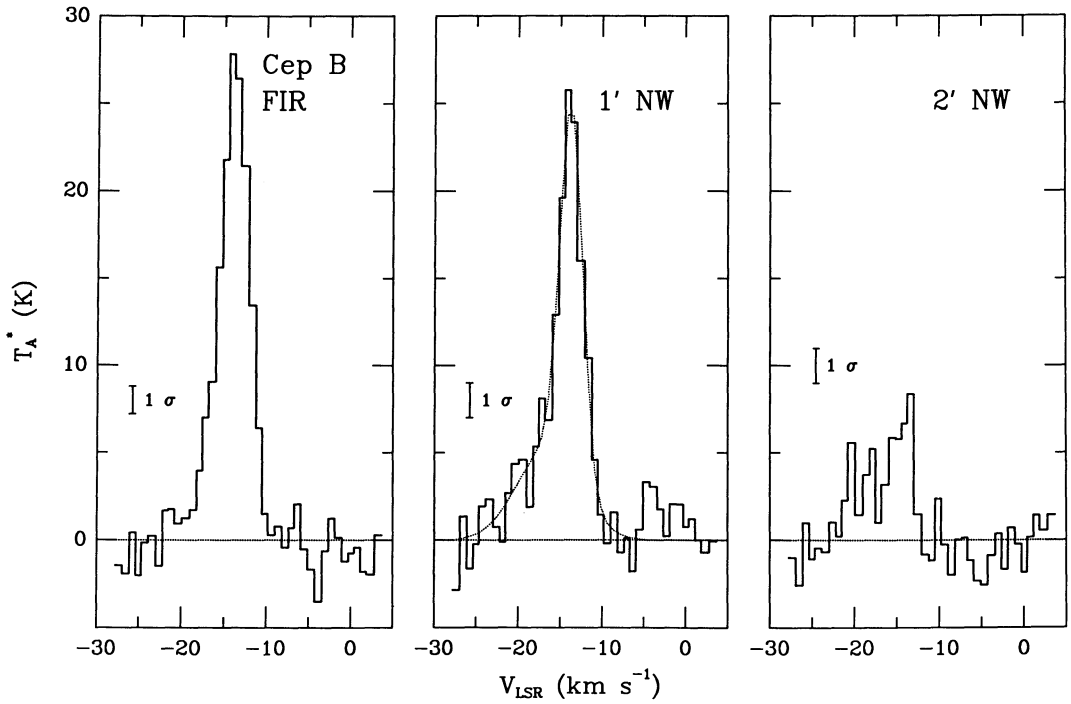

FIG. 4.—C II spectra in the region of Cep B: at the FIR peak (*left panel*), 1′ NW of the FIR peak (*middle panel*), and 2′ NW of the FIR peak (*right panel*). The dotted line in the central panel shows the fit of two Gaussian components to the spectrum. Integration times are 12 minutes at the FIR peak and 8 minutes for the other positions. The continuum has been subtracted from all spectra.

beam includes the radio peak seen by Felli *et al.* (1978), the integrated intensity of the C II has changed very little from its value at the FIR peak, and T_A^* has decreased only slightly. In contrast, the antenna temperature of the CO emission has decreased to ~ 5 K here, most likely because of the photodestruction of CO. On the other hand, the dust temperature of ~ 50 K is somewhat higher at this position than at the FIR peak.

The C II line 1′ NW of the FIR peak clearly consists of more than one component, and shows an extended blue wing. As shown in Figure 4*b*, the data are fitted well by two Gaussian components, with V_{LSR} of -13.8 and -16.5 km s^{-1}, and the former component 4 times as bright as the latter. The brighter and narrower component is probably the same as that seen at the FIR peak, while the broader and more blueshifted contribution, if it arises from a single source with a Gaussian line profile rather than asymmetric broadening from gradients within the cloud, represents a component of the photodissociated gas heretofore not identified in the molecular gas. Closer examination of the C II line profile from the FIR peak also reveals a slight blue asymmetry, and a fit of two Gaussians rather than one to the profile improves the reduced χ^2 value of the fit by 20%. The additional broad component then has a V_{LSR} of -16.5 ± 0.5 km s^{-1} and a FWHM of 6.0 ± 1.7 km s^{-1}, while the main component shifts to -13.6 ± 0.1 km s^{-1} with a width of 3.8 ± 0.2 km s^{-1}. The component at -16.5 km s^{-1}, obtained from an independent fit to the FIR peak data, is clearly the same as that present 1′ to the NW, although its existence could not be certified from just the slight (and statistically, not quite significant) blue asymmetry of the FIR peak spectrum.

Our C II data 2′ NW of the FIR peak, well within the H II region, suffer from a low signal-to-noise ratio, since the integrated intensity of the line has decreased more than fourfold from that at the peak. Only one Gaussian component can justifiably be fitted to the data, at -15.8 ± 0.5 km s^{-1} as shown in Table 1. However, if a second component at -16.5 km s^{-1} with variable amplitude and a FWHM of 7.5 km s^{-1} (deduced from the other two spectra, and fixed in this case) is forced into the fit, then the reduced χ^2 value improves by almost 25%, and the V_{LSR} of the primary component shifts to -13.8 ± 0.3 km s^{-1}, more consistent with that at the other two positions. The FWHM of the main component is 2.1 ± 0.8 km s^{-1}, significantly narrower than that observed closer to the molecular cloud.

Thus, all the data taken together tentatively indicate the presence of two velocity components in the C II emission of Cep B. The strongest component has a velocity of -13.8 km s^{-1}, which is similar to that of CO near the edge of the molecular cloud. The intensity and width of this component both decrease into the H II region. The second component at -16.5 km s^{-1}, whose existence must be considered somewhat tentative, has a more uniform intensity distribution, is more blueshifted, and is significantly wider than the main component. This weaker component may not be associated with the molecular cloud–H II region interface at all, since it does not appear to be peaked there, but may be related to the H II region S155 which shows a similar V_{LSR} in Hα emission.

A calculation of the expected C II integrated intensity from the H II region based on the parameters given by Felli *et al.* (1978) yields $\sim 5 \times 10^{-5}$ ergs cm^{-2} s^{-1} sr^{-1}, suggesting that some of the observed radiation at the 2′ NW position comes from hot, optically thin gas in the H II region. It is possible that the component with V_{LSR} near -16 km s^{-1} at all three locations in Cep B arises from this hot gas.

e) M17

The M17 region can be considered to be an extreme case of the H II region interacting with a molecular cloud, in which everything is on a larger and more intense scale than for the

sources previously discussed. The H II region (M17 or NGC 6618) forms a sharp interface with an extended and massive molecular cloud to the SW (M17 SW), and also with a less dense molecular cloud to the north (Gatley *et al.* 1979). The heating and ionization of the region is dominated by a cluster of up to 100 O and B stars, resulting in a very intense UV field in the region. The CO emission from M17 SW shows a very sharp decrease at the interface with the H II region, and the peak T_A^* is offset toward the ionization front relative to the position of peak CO column density (Lada 1976; Thronson and Lada 1983; Rainey *et al.* 1987). This morphology clearly suggests that the heating of the molecular gas is dominated by UV radiation from the external stars. The conclusion is supported by FIR continuum mapping (Gatley *et al.* 1979), which shows that the color temperature decreases monotonically into the cloud from ~85 K near the ionization front. The data also reveal a steep density gradient, with the H_2 density decreasing into the cloud. The FIR mapping suggests that the periphery of the molecular cloud is heated by UV and optical radiation from exciting stars and the nebula, while the core of the cloud is heated by infrared reradiation from embedded dust.

The molecular gas in M17 SW consists of at least two temperature components. The peak T_A^* for several low-J CO transitions which are expected to be optically thick indicate excitation temperatures of ~50 K. However, observations in higher-J CO transitions suggest excitation temperatures of up to a few hundred K for some locations (Harris *et al.* 1987). Line profiles in many CO transitions reveal complex structure, with several emission components, possible self-absorption, and significant changes on small spatial scales (Martin, Sanders, and Hills 1984; Rainey *et al.* 1987; Schulz and Krügel 1987; Harris *et al.* 1987). Modeling of the M17 cloud suggests a significant clumpiness both in the molecular and photodissociation regions (Martin, Sanders, and Hills 1984; Snell *et al.* 1984; Mundy *et al.* 1986, 1987; Genzel *et al.* 1988; Stutzki *et al.* 1988). Figure 1 of this latter reference illustrates the spatial relationship of the various components of M17.

C II in M17 was first observed by Russell *et al.* (1981), who found a uniform halo of emission extending for at least 12′. Stutzki *et al.* (1988) obtained a strip scan of the integrated intensity of the C II emission at somewhat higher spectral resolution and confirmed the large extent of low-level C II emission. The peak of the C II emission is offset into the molecular cloud relative to the peak in the radio continuum. The emission decreases smoothly to the SW into the bulk of the molecular material, but its distribution is complicated toward the NE because of the existence of a second ionization front/molecular cloud interface. A map of C II emission at 3.′7 resolution (Matsuhara *et al.* 1989) clearly shows the existence of two peaks in the C II integrated intensity associated with the two interfaces.

Our observations of M17 were performed at three positions: the peak of integrated C II emission observed by Stutzki *et al.* (1988), the C I peak seen by Genzel *et al.* (1988), and halfway between. With respect to the reference position of SAO 161357 at $\alpha(1950) = 18^h17^m34^s.5$, $\delta(1950) = -16°13'24''$, these three positions are at (−30, −15), (−90, −45), and (−60, −30), respectively, with the values in arcseconds, negative to the W and S. The three positions lie along a line perpendicular to the ionization front. The first position is ~1.′5 S of the C II peak shown in the map of Matsuhara *et al.* (1989). The last two positions approximately bracket the location of peak T_A^* in low-J CO lines, and the highest column density of CO lies within the beam at the third position. The direction of chop was along our three-position line perpendicular to the ionization front, with an amplitude of 10.′5. The spectra thus obtained are shown in Figure 5.

As can be seen from Figure 5, the line shapes of the C II are

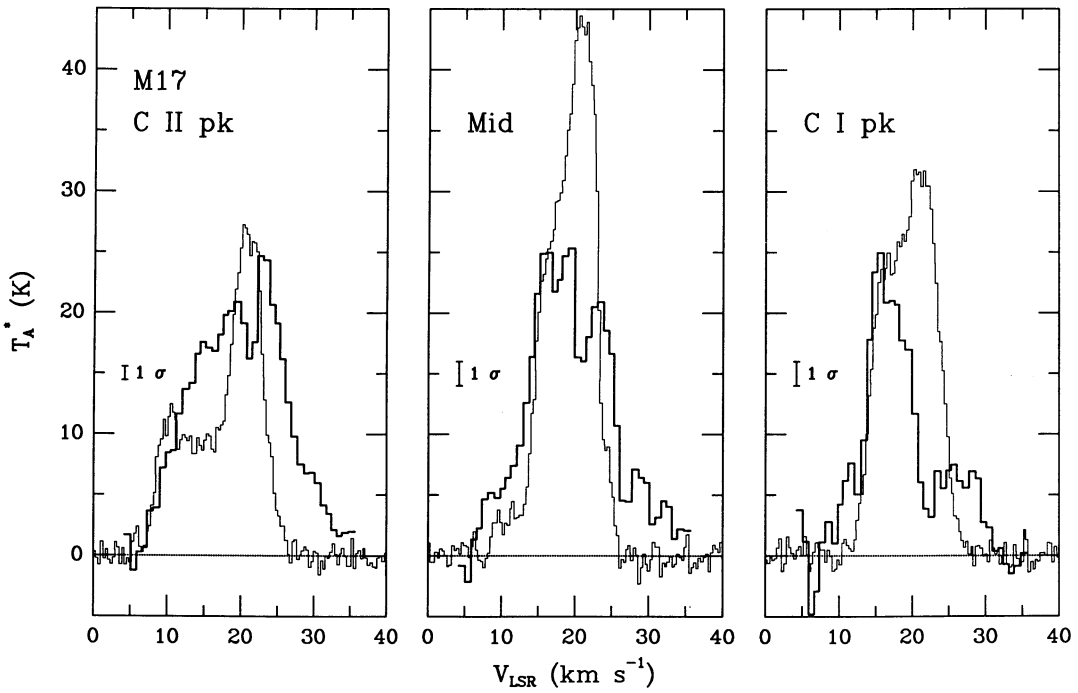

FIG. 5.—C II spectra (*heavy lines*) compared with CO $J = 2$–1 spectra (*light lines:* Stutzki *et al.* 1988) at three locations in M17: the C II peak of Stutzki *et al.* (*left panel*, 24 minutes integration), the C I peak of Genzel *et al.* 1988 (*right panel*, 8 minutes integration) and midway between (*middle panel*, 8 minutes integration). The continuum determined from the wide filter banks has been removed from all C II spectra. Some C II emission remains out to the limits of the high-resolution filter bank, as shown here.

complex at all three positions, with features suggesting the existence of at least one emission and one absorption (or "negative emission" from reference beam contamination) component. For comparison, the ^{12}CO $J = 2$–1 spectra at the same locations are also shown. The $^{12}C^{18}O$ spectra at the same three positions show relatively simple profiles, with that at the midposition (−60, −30) appearing to be a symmetric single Gaussian. The line profile at the C II peak (−30, −15) seems to have an extended blue wing, while that at the C I peak (−90, −45) shows evidence of an extended red wing. The coincidence of the central dip in the C II spectra with peak emission in the ^{12}CO $J = 2$–1 spectra and the single-peaked profile of the $C^{18}O$ data together suggest that the apparent C II dip may be produced by absorption in cooler or less dense foreground gas rather than the distinction between two separate velocity components.

The observed C II line shapes are probably somewhat complicated by the presence of emission in the "off-source" reference beam position. An estimate of emission in the reference beam can be obtained from the extended C II map of Matsuhara *et al.* (1989). The integrated intensities corrected for reference beam emission are 3.2×10^{-3} ergs cm^{-2} s^{-1} sr^{-1}, 3.1×10^{-3} ergs cm^{-2} s^{-1} sr^{-1}, and 2.0×10^{-3} ergs cm^{-2} s^{-1} sr^{-1} at (−30, −15), (−60, −30), and (−90, −45), respectively. These values are all consistent with those obtained from the scan of Stutzki *et al.* (1988) and the map of Matsuhara *et al.* (1989) when the larger beam size used for the latter is considered. The calculated minimum column density for optically thin radiation in the high-temperature limit yielding the stated intensities is $\sim 2 \times 10^{18}$ cm^{-2}.

We have attempted to obtain fits to the observed spectra assuming that they consist of a superposition of Gaussian emission components in both signal and reference beams. The best fits obtained in this manner are shown as the dotted curves in Figure 6, and the parameters of these fits are presented in Table 1. In each case, the fit is ∼25% worse than expected from statistical noise alone, indicating that our assumption of the number or shape of the components is probably not quite valid. The V_{LSR} was fixed in the fit to the spectrum in the C I peak (−90, −45) location, since the amplitudes of the absorption and emission components are highly coupled in this fit. An increase in the fitted amplitude of the emission component can be compensated by a similar increase in the amplitude of the absorption component, together with a shift to higher V_{LSR} and lower width for emission and to lower V_{LSR} and greater width for absorption, with the net result being fits with comparable values of χ^2 over a range of emission T_A^* of 20–40 K. Therefore the parameters associated with the fit at this particular position should be considered somewhat less certain.

The spectrum at the C II peak (−30, −15) with the highest signal-to-noise ratio can be fitted with one emission and two absorption components. There is also evidence in the other two M17 spectra for the existence of the second "absorption" component near $V_{LSR} = 18$ km s^{-1}. This dip (which in Figs. 5 and 6 appears near 16 km s^{-1} because it is superposed upon a sloping wing) is most likely caused by emission in the "off-source" beam located in the molecular cloud, since the ∼6 km s^{-1} width is typical for CO lines within the cloud. For example, the ^{12}CO $J = 2$–1 spectra of Stutzki *et al.* (1988) taken further SW from our source position (although not as far as our reference location) show the existence of a prominent emission at $V_{LSR} \sim 18$ km s^{-1}. Furthermore, the strength of the 18 km s^{-1} C II component decreases toward the SW, as expected from the C II map of Matsuhara *et al.* (1989) if the feature is produced by emission in the "off-source" reference beam in the molecular cloud.

The noticeable negative feature that appears near 21 km s^{-1} V_{LSR} in all three spectra may originate from the other "off-source" reference position near the second ionization front.

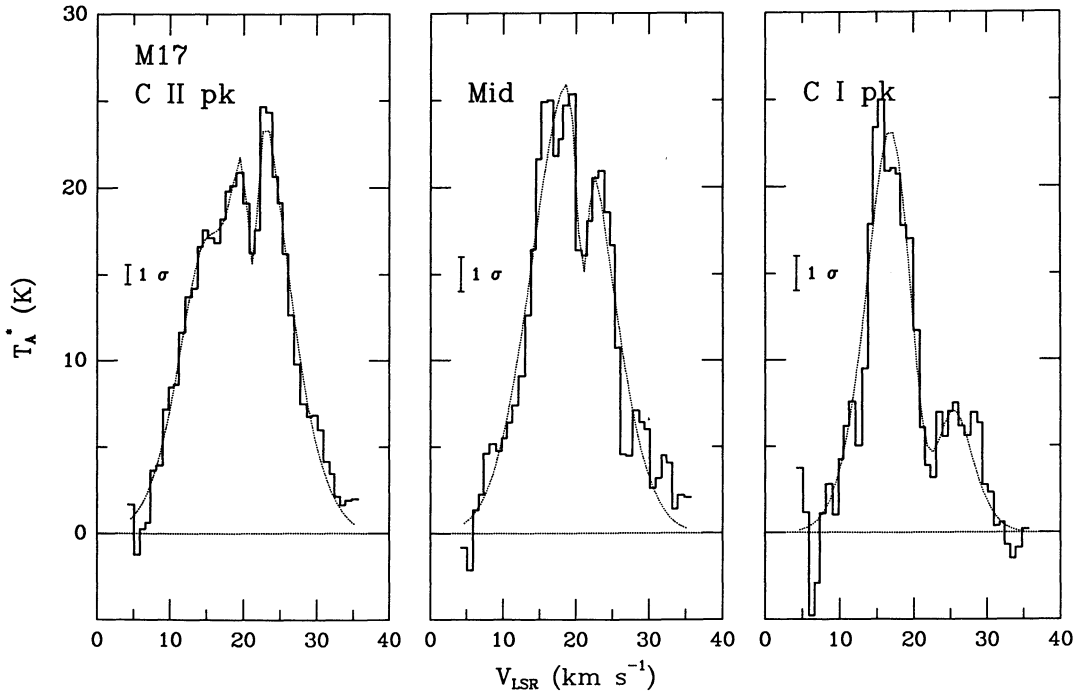

FIG. 6.—C II spectra at three locations in M17, as in Fig. 5. The dotted lines show the fits of a linear combination of Gaussian components to the spectra.

The integrated intensity of this feature increases toward the SW, as expected if this interpretation is valid. One clear conclusion from the C II spectra is that a region exists that produces very narrow C II features, of the order of 1.7 km s^{-1} FWHM, since no linear combination of wider Gaussians can produce the appearance of the sharp-edged absorptions seen in the data. This width is substantially smaller than typical C II line widths observed in other clouds.

The combined integrated intensity in "negative emission" or absorption features is 0.20, 0.06, and 0.41 of that seen in the main Gaussian component at the three positions observed. For comparison, the expected values from the Matsuhara *et al.* (1989) map are all near 0.25. The discrepancy in two of the locations suggests that the line profiles are not approximately Gaussian, that some of the "negative emission" is actually foreground absorption, or that some reference beam emission is not properly identified in the fitting procedure, perhaps because of the interdependence among fitted parameters. For example, we cannot detect the presence of emission in the reference beam with the same V_{LSR} and FWHM as the observed line. The width cannot be greater because of the absence of noticeable signals below continuum level, or much narrower because there are no obvious "absorption" features within the emission, apart from those already discussed.

One alternative interpretation for the narrow feature at 21 km s^{-1} is foreground absorption by cooler or less dense (and hence subthermally excited) material. Fits to the C II spectra under this assumption are equally as good as those obtained assuming reference beam contamination. The minimum optical depth and maximum brightness temperature, respectively, of the foreground absorber indicated by the fits are $\tau_{min} = 0.41 \pm 0.06$ and $T_{max} = 53 \pm 2$ K at $(-30, -15)$, $\tau_{min} = 0.51 \pm 0.15$ and $T_{max} = 48 \pm 3$ K at $(-60, -30)$, and $\tau_{min} = 1.7 \pm 0.2$ and $T_{max} = 31 \pm 2$ K at $(-90, -45)$. Unfortunately, because of our uncertainty of reference beam contamination, we cannot definitively say whether this "self-absorption" interpretation has any physical significance.

The brightness temperature of the main C II emission component deduced from the fit again appears to be similar to the dust temperature in the region, with no strong gradient indicated. As mentioned previously, however, the brightness temperature provides only a lower limit to the excitation temperature, not only because optical depth is unknown but also because reference beam emission with a comparable velocity profile would artificially lower the observed spectrum. The C II lines in M17 are considerably wider than molecular lines such as CO as well as C I observed in the same region, while from the fits the V_{LSR} appears lower by 1–2 km s^{-1}. The increased width of C II relative to CO could be explained by the turbulence in the photodissociated gas which may be streaming away from its point of origin. Also, given the possibility of line distortion from reference beam contamination and the spatially complex nature of the source, the apparent shift in V_{LSR} between CO and C II may not be real and would need to be confirmed through additional C II observations. Thus, the C II observations are not inconsistent with the clumpy model of Stutzki *et al.* (1988).

IV. SUMMARY AND CONCLUSIONS

We have observed the C II fine-structure line in five sources for which the ionization front/molecular cloud interface is viewed approximately edge-on. For most sources, the C II line has a simple Gaussian profile with a V_{LSR} similar to that seen in CO, but with a line width greater than that characterizing the molecular gas. Brightness temperatures corresponding to the observed antenna temperature are found to be similar to or somewhat higher than the dust temperature at all locations. The minimum C II column densities calculated by assuming optically thin radiation in the high temperature limit range from 2×10^{17} cm^{-2} to 2×10^{18} cm^{-2} for the sources discussed.

In the two sources for which the position of a well-established embedded source was observed (S140 and NGC 7538), the antenna temperature is somewhat lower and the line width is greater at the location of the embedded source than near the ionization front, thereby leading to very similar values of integrated intensity. Both of these sources show outflows in CO, and the wider lines could be due to an interaction of the outflow with the photodissociation region. All of the sources observed at the high resolution of 0.8 km s^{-1} show significant variations in the C II line profile on spatial scales $\lesssim 1'$, indicating rapid changes in physical conditions and kinematics on smaller scale sizes. Observations with a smaller beam size would be useful for determining the properties of photodissociation regions in more detail.

The sources observed, with the possible exception of M17, appear to have broadly similar characteristics. M17 has a higher brightness temperature, as might be expected from its much more intense UV field. The line shapes in M17 are very complex, with evidence for emission extended over more than 20′ which does not appear in other sources. There is also a narrow feature at 21 km s^{-1} in the M17 spectra which may be attributed to absorption from foreground gas with a low velocity dispersion. If this is truly absorption rather than "off-source" emission from a second ionization front in the region, then an optical depth of more than 1.7 is indicated.

There is evidence in some of the sources that part of the C II radiation arises from the H II region as well as from the interface with the molecular cloud. It is possible to distinguish between these two contributions to the net integrated intensity due to the side-illuminated geometry and also occasionally by different V_{LSR}, for which the high spectral resolution available with a heterodyne instrument is required. However, in cases of a face-on geometry, it may not be possible to separate the two components, and hence the interpretation of C II line intensities must be approached with caution, recognizing that two regions with greatly different physical characteristics (one hot, leading to very optically thin lines, and the other, considerably cooler, leading to potentially optically thick lines) could contribute to the observed integrated intensity.

The model of photodissociation regions developed by Tielens and Hollenbach (1985) predicts that the column density of C II in a photodissociation region is $\sim 2 \times 10^{18}$ cm^{-2} measured along the line of sight from the source of ionization, and that it should not be very sensitive to the UV flux and gas density, since it is determined predominantly by penetration depth of the ionizing UV photons. The column densities derived from our data for embedded sources (i.e., for a face-on view of the ionization front) are consistent with those expected on the basis of the model, given the range of possible UV fluxes, densities, and model parameters such as dust-to-gas ratio. The measured column density should be higher when observed at an angle to the direction of illumination, especially in the case of edge-on ionization fronts. However, column densities we derive for locations at which the ionization front is viewed approximately edge-on are generally very similar to

those derived for face-on ionization regions in the same source, rather than showing a clear increase due to superposition of emission along the line of sight. Unfortunately, the UV fluxes for the two geometries in any single source are significantly different, making meaningful comparisons impossible without more complete knowledge of the source morphology. In addition, the physical extent of the ionization front may be small in several of the observed sources, leading to underestimation of the peak C II column density due to beam dilution and non-optimum pointing.

The C II brightness temperatures are similar to dust temperatures in a variety of sources with line widths ranging from 3 to 14 km s^{-1}. Such a coincidence, resulting just from fortuitous combinations of a high excitation temperature and a low but variable optical depth, while possible, appears somewhat unlikely, and suggests that the C II lines from the edge-illuminated regions may be optically thick. However, there is insufficient dynamic range in the observed C II brightness temperatures to establish a clear relationship with dust temperature, and both temperatures are dependent upon the UV flux.

Whereas the presence of hot gas has been shown via high-J emission of CO and other higher excitation lines in sources such as Orion and M17, it should be recognized that these regions are exceptional, with much higher UV fluxes than for most of the sources discussed in this paper. Lower PDR temperatures might be expected for less UV heating, perhaps consistent with the most straightforward interpretation of the present data of optically thick, cool gas. However, if PDRs are intrinsically very clumpy such that beamfilling factors are less than one even for a side-illuminated geometry, then beam dilution could be significant in all of the sources, resulting in higher temperatures even if the lines are optically thick.

A definitive answer to the question of emission optical depth, and hence gas temperature in the photodissociation region, cannot be obtained from the present data. A good approach to the problem would be to observe the hyperfine components of ^{13}C II in several of the sources. Also, additional detailed observations of line profile changes across an ionization front and within the molecular clouds would be valuable for drawing more quantitative conclusions on the heating and cooling of photodissociation regions. Also, spectrally resolved observations of the 63 μm O I fine-structure line, which is expected to be somewhat optically thick in PDRs (Tielens and Hollenbach 1985), would be very useful for determining the temperature of these regions.

We are grateful to the staff of the Kuiper Airborne Observatory for their enthusiastic support during the course of these observations. We thank G. Stacey for providing us with access to CO $J = 2$–1 spectra prior to publication. This work was supported by NASA grant NAG 2–254.

REFERENCES

Bally, J., and Lada, C. J. 1983, *Ap. J.*, **265**, 824.
Bally, J., and Lane, A. P. 1982, *Ap. J.*, **257**, 612.
Beichman, C. A., Becklin, E. E., and Wynn-Williams, C. G. 1979, *Ap. J. (Letters)*, **232**, L47.
Betz, A. L., Boreiko, R. T., and Zmuidzinas, J. 1990, in preparation.
Betz, A. L., and Zmuidzinas, J. 1984, in *Proc. Airborne Astronomy Symposium*, ed. H. A. Thronson and E. F. Erickson (NASA CP-2353), p. 320.
Blair, G. N., Evans, II, N. J., Vanden Bout, P. A., and Peters, III, W. L. 1978, *Ap. J.*, **219**, 896.
Boreiko, R. T., Betz, A. L., and Zmuidzinas, J. 1988, *Ap. J. (Letters)*, **325**, L47.
Campbell, B., and Thompson, I. 1984, *Ap. J.*, **279**, 650.
Churchwell, E., and Bieging, J. H. 1982, *Ap. J.*, **258**, 515.
Cooksy, A. L., Blake, G. A., and Saykally, R. J. 1986, *Ap. J. (Letters)*, **305**, L89.
Crawford, M. K., Lugten, J. B., Fitelson, W., Genzel, R., and Melnick, G. 1986, *Ap. J. (Letters)*, **303**, L57.
Dickel, H. R., Dickel, J. R., and Wilson, W. J. 1981, *Ap. J. (Letters)*, **250**, L43.
Evans, II, N. J., Becklin, E. E., Beichman, C., Gatley, I., Hildebrand, R. H., Keene, J., Slovak, M. H., Werner, M. W., and Whitcomb, S. E. 1981, *Ap. J.*, **244**, 115.
Felli, M., and Harten, R. H. 1981, *Astr. Ap.*, **100**, 42.
Felli, M., Hjellming, R. M., and Cesaroni, R. 1987, *Astr. Ap.*, **182**, 313.
Felli, M., Tofani, G., Harten, R. H., and Panagia, N. 1978, *Astr. Ap.*, **69**, 199.
Fischer, J., Righini-Cohen, G., Simon, M., Joyce, R. R., and Simon, T. 1980, *Ap. J. (Letters)*, **240**, L95.
Fischer, J., Sanders, D. B., Simon, M., and Solomon, P. M. 1985, *Ap. J.*, **293**, 508.
Gatley, I., Becklin, E. E., Sellgren, K., and Werner, M. W. 1979, *Ap. J.*, **233**, 575.
Genzel, R., Harris, A. I., Jaffe, D. T., and Stutzki, J. 1988, *Ap. J.*, **332**, 1049.
Glassgold, A. E., and Langer, W. D. 1974, *Ap. J.*, **193**, 73.
Goldsmith, P. F., and Linke, R. A. 1981, *Ap. J.*, **245**, 482.
Harris, A. I., Stutzki, J., Genzel, R., Lugten, J. B., Stacey, G. J., and Jaffe, D. T. 1987, *Ap. J. (Letters)*, **322**, L49.
Hayashi, M., Hasegawa, T., Omodaka, T., Hayashi, S. S., and Miyawaki, R. 1987, *Ap. J.*, **312**, 327.
Hayashi, M., Omodaka, T., Hasegawa, T., and Suzuki, S. 1985, *Ap. J.*, **288**, 170.
Keene, J., Blake, G. A., Phillips, T. G., Huggins, P. J., and Beichman, C. A. 1985, *Ap. J.*, **299**, 967.
Lada, C. J. 1976, *Ap. J. Suppl.*, **32**, 603.
Langer, W. D. 1976, *Ap. J.*, **206**, 699.
Lester, D. F., Harvey, P. M., Joy, M., and Ellis, H. B. Jr. 1986, *Ap. J.*, **309**, 80.
Linsky, J. L. 1973, *Ap. J. Suppl.*, **25**, 163.
Mampaso, A., Phillips, J. P., Vilchez, J. M., Pismis, P., and Riera, A. 1989, *Astr. Ap.*, **220**, 235.
Martin, R. N., and Barret, A. H. 1978, *Ap. J. Suppl.*, **36**, 1.
Martin, H. M., Sanders, D. B., and Hills, R. E. 1984, *M.N.R.A.S.*, **208**, 35.
Matsuhara, M., *et al.* 1989, *Ap. J. (Letters)*, **339**, L67.
Melnick, G., Stacey, G. J., Viscuso, P. J., and Fuller, C. E. 1986, *Ap. J.*, **303**, 638.
Mundy, L. G., Evans, II, N. J., Snell, R. L., and Goldsmith, P. F. 1987, *Ap. J.*, **318**, 392.
Mundy, L. G., Snell, R. L., Evans, II, N. J., Goldsmith, P. F., and Bally, J. 1986, *Ap. J.*, **306**, 670.
Petersen, F. R., Scalabrin, A., and Evenson, K. M. 1980, *Int. J. Infrared Millimeter Waves*, **1**, 111.
Phillips, T. G., and Huggins, P. J. 1981, *Ap. J.*, **251**, 533.
Phillips, T. G., Knapp, G. R., Huggins, P. J., Werner, M. W., Wannier, P. G., Neugebauer, G., and Ennis, D. 1981, *Ap. J.*, **245**, 512.
Plambeck, R. L., Snell, R. L., and Loren, R. B. 1983, *Ap. J.*, **266**, 321.
Rainey, R., White, G. J., Gatley, I., Hayashi, S. S., Kaifu, N., Griffin, M. J., Monteiro, T. S., Cronin, N. J., and Scivetti, A. 1987, *Astr. Ap.*, **171**, 252.
Russell, R. W., Melnick, G., Gull, G. E., and Harwit, M. 1980, *Ap. J. (Letters)*, **240**, L99.
Russell, R. W., Melnick, G., Smyers, S. D., Kurtz, N. T., Gosnell, T. R., Harwit, M., and Werner, M. W. 1981, *Ap. J. (Letters)*, **250**, L35.
Sargent, A. I. 1977, *Ap. J.*, **218**, 736.
Schulz, A., and Krügel, E. 1987, *Astr. Ap.*, **171**, 297.
Schwartz, P. R., Thronson, H. A., Jr., Lada, C. J., Smith, H. A., Glaccum, W., Harper, D. A., and Knowles, S. H. 1983, *Ap. J.*, **271**, 625.
Scoville, N. Z., Sargent, A. I., Sanders, D. B., Claussen, M. J., Masson, C. R., Lo, K. Y., and Phillips, T. G. 1986, *Ap. J.*, **303**, 416.
Snell, R. L., Huang, Y.-L., Dickman, R. L., and Claussen, M. J. 1988, *Ap. J.*, **325**, 853.
Snell, R. L., Mundy, L. G., Goldsmith, P. F., Evans, II, N. J., and Erickson, N. R. 1984, *Ap. J.*, **276**, 625.
Stutzki, J., Stacey, G. J., Genzel, R., Harris, A. I., Jaffe, D. T., and Lugten, J. B. 1988, *Ap. J.*, **332**, 379.
Takano, T. 1986, *Ap. J.*, **303**, 349.
Thronson, H. A., Jr., and Lada, C. J. 1983, *Ap. J.*, **269**, 175.
Thronson, H. A., Jr., Smith, H. A., Lada, C. J., Glaccum, W., Harper, D. A., Loewenstein, R. F., and Smith, J. 1984, *M.N.R.A.S.*, **207**, 659.
Tielens, A. G. G. M., and Hollenbach, D. 1985, *Ap. J.*, **291**, 722.
Werner, M. W., Becklin, E. E., Gatley, I., Matthews, K., and Wynn-Williams, C. G. 1979, *M.N.R.A.S.*, **188**, 463.
Wramdemark, S., and Lynga, G. 1987, *IAU Symposium 115, Star-Forming Regions*, ed. M. Peimbert and J. Jugaku (Dordrecht: Reidel), p. 211.
Zmuidzinas, J., Betz, A. L., and Boreiko, R. T. 1989, *Infrared Phys.*, **29**, 119.

A. L. Betz and R. T. Boreiko: Space Sciences Laboratory, University of California, Berkeley, CA 94720

J. Zmuidzinas: Astronomy Department, University of Illinois, 1011 West Springfield Avenue, Urbana, IL 61801